Received: 7 September 2025 | Revised: 21 November 2025 | Accepted: 30 November 2025

DOI: 10.1111/bph.70316

RESEARCH ARTICLE

Induction of IL-9-producing CD8$^+$ T cells by ascochlorin derivatives

Natsumi Imano[1] | Mikako Nishida[2] | Miho Tokumasu[1] | Weiyang Zhao[1] | Nahoko Yamashita[2] | Heiichiro Udono[2]

[1]Department of Immunology, Okayama University Faculty of Medicine, Dentistry and Pharmaceutical Sciences, Kita-ku, Okayama, Japan

[2]Department of Metabolic Immune Regulation, Okayama University Faculty of Medicine, Dentistry and Pharmaceutical Sciences, Kita-ku, Okayama, Japan

Correspondence
Heiichiro Udono, Department of Metabolic Immune Regulation, Okayama University Faculty of Medicine, Dentistry and Pharmaceutical Sciences, 2-5-1 Shikata-cho, Kita-ku, Okayama 700-8558, Japan.
Email: udono@cc.okayama-u.ac.jp

Funding information
Japan Society for the Promotion of Science, Grant/Award Numbers: 17K19598, 18H04033, 24K02326; JST SPRING, Grant/Award Number: JPMJSP2126

Background and Purpose: Ascochlorin (ASC) is an antiviral antibiotic from the fermented broth of *Ascochyta viciae* which exerts an inhibitory effect to cancers. Its impact on immune cells has not been examined. In this study, we obtained ASC derivatives with less cytotoxicity and determined whether they affected T cells, indicating possible immune-mediated antitumour effects.

Experimental Approach: Newly synthesised ASC derivatives were screened for inhibitory effects on T-cell antigen receptor (TCR)-stimulated proliferative responses using murine CD4$^+$ and CD8$^+$ T cells. Two compounds were identified that exhibited >10-fold less toxicity compared with ASC. N184, the less toxic of the two, was analysed for its in vivo antitumour effects, and in vitro effects on CD8$^+$ T-cell proliferation, survival, cytokine production and exhaustion, using microscopy, qPCR and flow cytometry.

Key Results: N184 induced limited IL-9 production in CD8$^+$ T cells following TCR stimulation, thereby improving cell survival. It also enhanced cytokine production in the late phase of proliferation and suppressed the induction of exhaustion. N184 suppressed tumour growth in mice in a CD8$^+$ T cell-dependent manner. The effect was partially prevented by an IL-9-neutralising antibody.

Conclusion and Implications: N184 induces differentiation of IL-9-producing CD8$^+$ T cells in vitro and elicits antitumour immunity in an IL-9-dependent manner.

KEYWORDS
ascochlorin derivative, CD8 positive T lymphocytes, cell survival, IFN-γ, interleukin-9, Tc9, tumour immunity

1 | INTRODUCTION

Ascochlorin (ASC) is an antibiotic, discovered in the fermented broth of *Ascochyta viciae* in a search for antibiotics with antiviral activity (Tamura et al., 1968) and the strain was re-identified as the ascofuranone-producing fungus *Acremonium sclerotigenum* (Hijikawa et al., 2017). Although no antiviral effect has been observed, ASC exerts a direct inhibitory effect to various cancers. Intraperitoneal

Abbreviations: Bcl2, B-cell/CLL lymphoma 2; Bcl-xL, B-cell lymphoma-extra large; FCS, fetal calf serum; FITC, fluorescein isothiocyanate; Fucci, fluorescent ubiquitination-based cell cycle indicator; Mcl1, myeloid cell leukaemia-1; PMA, *phorbol 12-myristate 13-acetate*; qPCR, quantitative polymerase chain reaction; RPMI, Roswell Park Memorial Institute; Tc, cytotoxic T lymphocyte; TCR, T-cell antigen receptor; TILs, tumour infiltrating lymphocytes.

Natsumi Imano and Mikako Nishida equally contributed to this study.

injection of ASC resulted in a modest antitumour effect to EHRLICH tumour ascites in mice (Tamura et al., 1968). ASC is an inhibitor of Complex III in the mitochondrial electron transport chain (Berry et al., 2010) and activated p53 (Jeong et al., 2009; Khutornenko et al., 2010), inducing cell cycle G1-arrest through cMyc inhibition-mediated p21 induction in a p53-independent manner (Jeong et al., 2018; Jeong & Chang, 2010). ASC reduced renal cell carcinoma invasion through the inhibition of activator protein-1 (AP-1)-dependent matrix metalloproteinases-9 (**MMP-9**) expression (Hong et al., 2005). AP-1 inhibition by ASC resulted in cytotoxicity to oestrogen receptor (**ER**)-negative human breast cancer cells (Sakaguchi et al., 2005). ASC inhibited epithelial growth factor (**EGF**)-mediated hypoxia-inducible factor-1α (HIF-1α) activation and tumour-angiogenesis in cervical cancer (Jeong et al., 2012). It also inhibited focal adhesion kinase (FAK) and **JAK2**/**STAT3** signalling, which resulted in the suppression of MMP-2-mediated migration of glioma cells (Cho et al., 2018). STAT3 inhibition by ASC suppressed hepatocellular carcinoma (HCC) growth (Dai et al., 2015). 4-O-methylascochlorin (MAC) and Ilicicolin C, both ASC derivatives, inhibited **mTOR** to suppress cancer cell progression (Gan et al., 2025; Seok et al., 2018).

IL-9 was originally identified as a T-cell growth factor (P40 molecule) derived from the supernatants of the concanavalin A (ConA)-stimulated mouse helper T-cell lines (Uyttenhove et al., 1988). Studies using tumour-specific adoptive immunotherapy models indicated that IL-9-producing $CD8^+$ T cells (Tc9) were more potent than Tc1 cells in eliciting antitumour responses through their long-term persistence in vivo (Lu, Hong, et al., 2014). Tumour-specific Th9 cells also promoted a strong antitumour response (Chen et al., 2024; Lu et al., 2012, 2018; Sek et al., 2021). IL-9 neutralising Ab injection enhanced B16 melanoma lung metastasis with decreased migration of memory T cells and dendritic cells in the lung (Lu et al., 2012). The P40 molecule was characterised as a mast cell growth-enhancing factor with complete sequence homology to human IL-9 (Moeller et al., 1990). Exogenous recombinant IL-9 inhibited tumour growth in recombination activating gene $(Rag1)^{-/-}$ mice, and this effect was abrogated in mast cell-deficient mice, suggesting the involvement of mast cells in the antitumour effect (Purwar et al., 2012).

In this study, we examined ASC's unexplored effects on immune cells, focusing on whether they affected T cells, thus indicating the potential of immune-mediated anti-tumour effects. We successfully identified two compounds that are 10-fold less toxic compared with ASC in T-cell proliferation tests following T-cell antigen receptor (TCR) stimulation. These two compounds significantly improved the survival of mouse $CD8^+$ T cells during proliferation. Moreover, both compounds induced mouse $CD8^+$ T cells to produce IL-9, albeit at a low level. The administration of N184, the less toxic of the two compounds, to tumour-bearing mice inhibited tumour growth in a concentration-dependent manner. This suppression was completely abolished by depleting $CD8^+$ T cells and partially by treatment with an IL-9-neutralising antibody. Our results indicate that certain ASC-derivatives, such as N184, elicit antitumour responses by inducing IL-9-producing $CD8^+$ T cells.

What is already known

- Ascochlorin and its derivatives exert antitumour effects through direct inhibition of cancer cells.

What does this study add

- The newly synthesised ascochlorin derivative N184 enhances the viability and function of $CD8^+$ T cells.
- N184 induces $CD8^+$ T-cell differentiation to the Tc9-like subset and antitumour effect in vivo.

What is the clinical significance

- N184 may have potential applications in immunotherapy for solid tumours, including cell therapy.

2 | METHODS

2.1 | Compounds

ASC and its derivatives (N184, HK-11, N104, N170, N174, N200 and N201) were kindly provided by NRL Pharma., Inc (Tokyo, Japan). The synthesis and physicochemical characteristics of these compounds are described in United States Patent No. US 10,968,186 B2. Chemical structures were designated by ChemSketch (ACD/Labs, Canada).

2.2 | Mice

C57BL/6J (B6) mice (female and male, 8- to 11-week old) and Balb/c mice (female, 8-week-old) purchased from Japan SLC, Inc. (Hamamatsu, Japan), and CB17/IcrJcl-$Prkdc^{scid}$ mice (female, 8-week-old) purchased from CLEA Japan, Inc. (Fujinomiya, Japan) were used for the experiments. All animals were maintained under specific pathogen-free conditions in the animal facility of Okayama University. All animal procedures were approved by the Institutional Animal Care and Use Committee of Okayama University Graduate School of Medicine (OKU-2022757). Animal studies are reported in compliance with the ARRIVE guidelines (Percie du Sert et al., 2020) and with the recommendations made by the British Journal of Pharmacology (Lilley et al., 2020).

2.3 | Tumour cell lines

Ovalbumin (OVA) gene-transfected B16 mouse melanoma MO5 cells, mouse fibrosarcoma MethA cells and mouse colon carcinoma CT26 cells were used for tumour assays as previously described (Eikawa

et al., 2015; Nishida et al., 2021). B16-fucci cells, which express a fluorescent cell-cycle reporter as a control, and B16-fucci cells, which lack the intracellular domain of **IFNGR1** (B16 fucci-δIC) (Matsushita et al., 2015) were also used. The cells were cultured in Roswell Park Memorial Institute (RPMI)-1640 medium (Thermo Fisher Scientific, MA, USA) supplemented with 10% fetal calf serum (FCS) (Biowest, Nuaille, France), 1 × modified eagle medium (MEM) nonessential amino acids (NEAA) (Gibco, MA, USA), 2 mM L-glutamine (Sigma-Aldrich, MA, USA), 1 mM sodium pyruvate (Wako, Osaka, Japan) and 50 μM 2-mercaptoethanol (2-ME) (Wako) at 37°C in a 5% CO_2 incubator. MO5 cells were cultured with G418 (Roche, Basel, Switzerland) to maintain ovalbumin (OVA)-expression. MethA cells were maintained in mouse ascites fluid.

2.4 | In vitro CD4$^+$ and CD8$^+$ T-cell culture

Mice were killed by cervical dislocation and their spleens were then removed. Splenic CD4$^+$ and CD8$^+$ T cells were isolated using iMag anti-mouse CD4 or CD8α particles and a BD™ IMag Cell Separation magnet (BD Biosciences, NJ, USA) at 90% purity. Isolated CD4$^+$ and CD8$^+$ T cells were stimulated with 1 μg mL^{-1} immobilised anti-CD3ε (145-2C11) (Cat#: 16-0031-86, RRID:AB_468847, Invitrogen, MA, USA) and 2 μg mL^{-1} soluble anti-CD28 monoclonal antibodies (mAbs) (37.51) (Cat#: 16-0281-86, RRID:AB_468923, Invitrogen, MA, USA) in a 96-well plate at a density of 5–7 × 10^4 cells per well in 200 μl of culture medium. ASC and its derivatives were dissolved in DMSO (Wako) and added to the medium at varying concentrations either at the beginning of culture or, for N184 (10 μM), at 24, 48 or 72 h after culture initiation. To induce Tc9 subset, CD8$^+$ T cells were cultured with Tc9-polarised medium supplemented with recombinant murine IL-4 (10 ng ml^{-1}, Pepro Tech, NJ, USA), recombinant murine TGF-β (1 ng ml^{-1}, BioLegend, CA, USA) and anti-IFNγ mAb (10 μg ml^{-1}, Cat# BE0055, RRID:AB_1107694, Bio X Cell, NH, USA) (Lu, Hong, et al., 2014; Ma et al., 2018).

For long-term culture experiments, CD8$^+$ T cells were incubated with 10 μM N184 or Tc9-polarised medium for 7 days. The cells were harvested, and the culture medium was removed by centrifugation. N184-treated CD8$^+$ T and Tc9 cells were divided into two groups [N184(−) and N184(+)] or [Tc9(−) and Tc9(+)] and subjected to secondary stimulation with anti-CD3 and anti-CD28 mAbs until day 28.

2.5 | Cytotoxicity assay

The cytotoxic effect of the compounds in MO5 cells and T cells was determined using the Cell Counting Kit-8 (CCK-8) (DOJINDO, Kumamoto, Japan). MO5 cells were seeded into 96-well plates at a density of 4 × 10^3 cells per well in 200 μl RPMI-1640 medium. MO5, CD4$^+$ and CD8$^+$ T cells were cultured in medium containing the compounds at 1, 5 or 10 μM. CCK-8 solution (10 μl per well) was added and incubated at 37°C for 2–4 h. The absorbance was measured at 450 nm using a POWER SCAN HT microplate reader (Sumitomo Dainippon Pharma Co., Ltd, Osaka, Japan). Relative cell viability was calculated using the following formula: (As − Ab)/(Ac − Ab) × 100 (%) (As: The absorbance of the sample, Ab: The absorbance of the blank, Ac: The absorbance of the untreated control).

2.6 | Cell viability assay

To evaluate the cell viability of CD4$^+$ and CD8$^+$ T cells, live (A) and dead (B) cell numbers were subject to trypan blue (Nacalai Tesque, Kyoto, Japan) staining. The cells were counted under a light microscope (OLYMPUS CX21) (OLYMPUS, Tokyo, Japan). Cell viability was calculated as follows: A/(A + B) × 100 (%). For the culture supernatant (sup) exchange experiment, CD8$^+$ T cells were cultured with 10 μM N184, and 90% of the culture supernatant was exchanged between the control and N184-treated groups on day 3. For the sham control, the culture supernatant was removed and added back to the original wells.

2.7 | Neutralising antibody treatment in vitro

To inhibit cytokine activity in vitro, 10 μg mL^{-1} of anti-IL-2 (JES6-1A12) (Cat #: A2138 Selleck Chemicals, TX, USA), anti-IL-9 (Cat# BE0181, RRID:AB_10950648, Bio X Cell) or anti-IL-15 (Cat# 16-7154-81, RRID:AB_469238, Thermo Fisher Scientific) mAb were added to the culture supernatant and incubated for 30 min at room temperature (RT). The supernatant was either exchanged between the control and the N184-treated groups or added back to the original wells on day 3. Alternatively, CD8$^+$ T cells were cultured in medium containing 10 μM N184 and 10 μg mL^{-1} of anti-IL-9 (Cat# BE018, RRID:AB_10950648, Bio X Cell) or anti-IFNγ mAb (Cat# BE0055, RRID:AB_1107694, Bio X Cell) from the beginning of culture.

2.8 | Tumour growth assay and in vivo treatment

Mice were intradermally inoculated with MO5, MethA, CT26, B16-fucci or B16 fucci-δIC cells (2.0 × 10^5 in 0.2 ml FCS-free RPMI-1640 medium) with a 27-gauge needle on day 0. On day 7 following tumour injection, the mice were administered N184 orally every other day at concentrations prepared by serial 1/3 dilution from the initial dose of 100 mg kg^{-1} to evaluate dose response. To evaluate the effective therapeutic initiation time of N184 treatment, tumour-bearing mice were administered N184 at a dose of 100 mg kg^{-1} starting on days 7, 10, and 13 after tumour inoculation. N184 was dissolved in 95% polyethylene glycol 400 (Wako) plus 5% polysorbate 80 (Wako). In vivo depletion of CD8$^+$ T cells was achieved by intraperitoneal injection of anti-CD8 mAb (anti-Lyt-2.2), which was prepared from 50 μl of ascitic fluid diluted in 150 μl PBS on days 6 and 10 following tumour inoculation, as previously described (Eikawa et al., 2015). In vivo neutralisation of IL-9 was achieved by intraperitoneal injection of 300 μg per animal anti-IL-9 mAb (Cat# BE018, RRID:AB_10950648, Bio X Cell) diluted in PBS, which was administered every 3 days beginning on day 7, as described

previously (Lu, Hong, et al., 2014). Metformin hydrochloride (5 mg mL^{-1}) (Tokyo Chemical Industry, Tokyo, Japan) was dissolved in drinking water and provided ad libitum to tumour-bearing mice from day 7 (Eikawa et al., 2015). The long (a) and short (b) diameters of the tumour were measured using Vernier callipers, and tumour volume (V) was calculated using the following formula: $V = a \times b^2/2$.

2.9 | Tumour-infiltrating lymphocytes (TIL) analysis

B6 mice were intradermally inoculated with 2.0×10^5 MO5 cells. The tumour tissues were dissected from the mice, after killing by cervical dislocation, on day 13, thus, 6 days after initiation of administrating 100 mg kg^{-1} dose of N184 and minced into small pieces in RPMI-1640 medium. TILs were harvested from the minced tumour tissues using the Medimachine system (AS ONE). All cells including TILs and tumour cells were stained with fluorescence-labelled antibodies and subjected to Flow cytometry analysis as previously described (Eikawa et al., 2015; Nishida et al., 2021).

2.10 | SDS-PAGE and Immunoblotting

Cells (1.0×10^6) were suspended in 250 μl of RIPA buffer (Nacalai Tesque) containing 1 mM PMSF (Wako), and incubated at 4°C for 30 min. The supernatant was mixed with 5 × SDS sample buffer containing 2-ME and denatured by boiling for 10 min. Samples were subjected to sodium dodecyl sulfate-polyacrylamide gel electrophoresis (SDS-PAGE), and the separated proteins were transferred onto polyvinylidene fluoride (PVDF) membranes (Merck Millipore, MA, USA). The membranes were blocked with 5% skim milk (Wako) in TBS-T (Tris-buffered saline [TBS] containing 0.05% Tween-20) at RT for 1 h. Primary antibodies (1:1000) were diluted in blocking buffer and incubated either overnight at 4°C or for 1 h at RT. Horseradish peroxidase (HRP)-conjugated secondary antibodies (1:2000) were incubated at RT for 1 h. After each incubation step, the polyvinylidene difluoride (PVDF) membranes were washed three times with TBS-T for 5 min. The protein bands were visualised using SuperSignal™ West Pico PLUS Chemiluminescent Substrate (Thermo Fisher Scientific) and detected with a ChemiDoc XRS+ (Bio-Rad, CA, USA). Anti-Bcl2 (Cat# 68103-1-Ig, RRID:AB_2923635), anti-Bcl-xL (Cat# 66020-1-Ig, RRID:AB_11042315), anti-Mcl1 (Cat# 66026-1-Ig, RRID:AB_11041711) and HRP-conjugated goat anti-mouse IgG (Cat# SA00001-1, RRID:AB_2722565) were purchased from Proteintech (USA). Anti-Phospho-Bad (Ser112) (Cat# 5284, RRID:AB_560884) and HRP-conjugated goat anti-rabbit IgG (Cat# 7074, RRID:AB_2099233) were purchased from Cell Signalling Technology (MA, USA). Anti-β-actin (Cat# bs-0061R, RRID:AB_10855480) was obtained from Bioss Antibodies (MA, USA).

2.11 | RNA extraction and quantitative reverse transcription-polymerase chain reaction (RT-PCR) analysis

Cells were harvested, resuspended in FCS-free RPMI-1640 medium containing 1.25 ng mL^{-1} phorbol 12-myristate 13-acetate (PMA) (Sigma-Aldrich) and 50 nM ionomycin (Sigma-Aldrich), and incubated at 37°C for 3 h. For IL-9 detection during IFNγ blockade, $CD8^+$ T cells were stimulated with PMA and ionomycin in the presence of 10 μg mL^{-1} anti-IFNγ mAb (Cat# BE0055, RRID:AB_1107694, Bio X Cell). Total RNA was extracted using ISOGEN II (Nippon Gene, Tokyo, Japan) based on the manufacturer's instructions. The RNA concentration was measured and adjusted to 1 μg μL^{-1} using a Nanodrop Lite spectrophotometer (Thermo Fisher Scientific). Complementary DNA (cDNA) was synthesised from 1 μg total RNA using the PrimeScript™ II 1st strand cDNA Synthesis Kit (TAKARA, Kusatsu, Japan). The cDNA was combined with forward and reverse primers and the Luna Universal qPCR Master Mix (New England Biolabs, MA, USA), based on the manufacturer's instructions. Quantitative RT-PCR was carried out using a StepOne plus™ real-time PCR system (Thermo Fisher Scientific). The primers used for qPCR are listed in Table 1 and were obtained from Thermo Fisher Scientific.

2.12 | Flow cytometry analysis

Approximately 1.0×10^6 cells were harvested for flow cytometry analysis. For cell surface staining, the cells were incubated with fluorescent-conjugated antibodies (1:50), diluted in PBS

TABLE 1 Primers used in this study.

Target genes	Forward (5′-3′)	Reverse (3′-5′)
Il2	TTTCAATTGGAAGATGCTGA	ATTGGCACTCAAATGTGTTG
Il7	ATCACAAGGCACACAAACAC	CTCTTTAGGAAACATGCATCA
Il9	CCTAAAGAACATCACGTGTCC	CCCAGGAGACTCTTCAGAAA
Il15	CTTGCAAACAGCACTCTGTC	GCTTTGCAAAAACTCTGTGA
Ifng	GGATGCATTCATGAGTATTGC	CCTTTTCCGCTTCCTGAGG
Il4	AGAGACTCTTTCGGGCTTTT	GCTTTCCAGGAAGTCTTTCA
Gzmb	CAAAGACCAAACGTGCTTC	TGGAGGTGAACCATCCTTAT
Prf1	AATATCAATAACGACTGGCGTGT	CATGTTTGCCTCTGGCCTA
ACTB	AAGGCCAACCGTGAAAAGAT	GTGGTACGACCAGAGGCATAC

supplemented with 2 mM EDTA and 0.5% BSA in the dark at 4°C for 30 min. For intracellular cytokine staining, the cells were incubated in FCS-free RPMI−1640 medium containing GolgiStop, a Protein Transport Inhibitor containing Monensin (BD Biosciences, NJ, USA), with or without 1.25 ng mL^{-1} PMA and 50 nM Ionomycin at 37°C for 6 h. For cytokine blockade, cells were stimulated with PMA and ionomycin in the presence of 10 μg mL^{-1} anti-IFNγ (Cat# BE0055, RRID:AB_1107694, Bio X Cell) or anti-IL-9 mAb (Cat# BE018, RRID:AB_10950648, Bio X Cell). For dead cell staining, $CD8^+$ T cells were incubated with the Zombie Violet Fixable Viability Kit (1:1000) (BioLegend) diluted in PBS at RT for 20 min before surface staining. The cells were stained with fluorescence-conjugated anti-CD3ε and anti-CD8α Abs in the dark at 4°C for 30 min. The cells were fixed and permeabilised using a Fixation/Permeabilisation kit (BD Biosciences) in the dark at 4°C for 20 min, followed by intracellular staining with fluorescent-conjugated antibodies (1:50) diluted in perm/wash buffer in the dark at 4°C for 30 min. The samples were analysed using a fluorescence-activated cell sorting (FACS) Canto II (BD Biosciences) or a CytoFlexS (Beckman Corter, CA, USA) with FlowJo software (version 10) (BD Biosciences). BV510 anti-mouse CD3 (Cat# 100234, RRID:AB_2562555), APC/Fire™ anti-mouse CD8α (Cat# 100766, RRID:AB_2572113), FITC anti-mouse IFNγ (Cat# 505806, RRID:AB_315400), PE anti-mouse TNFα (Cat# 506306, RRID:AB_315427), PE/Cy7 anti-mouse IL-2 (Cat# 503832, RRID:AB_2561750), APC anti-mouse IL-9 (Cat# 514106, RRID:AB_2562528), APC anti-mouse TIM3 (Cat# 134007, RRID:AB_2562997), PE/Cy7 anti-mouse PD-1 (Cat# 109109, RRID:AB_572016), FITC anti-mouse/human CD44 (Cat# 103006, RRID:AB_312957), allophycocyanin/cyanine7 (APC/Cy7) anti-CD44 (Cat# 103027, RRID:AB_830784), brilliant violet 421 (BV421) anti-mouse CD62L (Cat# 104436, RRID:AB_2562560), PE/Cy7 anti-CD107a (Cat# 121619, RRID:AB_2562146), APC anti-IL-2 (Cat# 503809, RRID:AB_315303), Pacific blue anti-TNFα (Cat# 506318, RRID:AB_893639) and PE/Cy5 anti-CD8α (Cat# 100710, RRID:AB_312749) were purchased from BioLegend. FITC anti-Bcl-2 (Cat# 11-6992-42, RRID:AB_10734060) was obtained from Thermo Fisher Scientific. The Immuno-related procedures used comply with the recommendations made by the British Journal of Pharmacology (Alexander et al., 2018).

2.13 | Statistical analysis

Data and statistical analysis complied with the recommendations of the *British Journal of Pharmacology* on experimental design and analysis in pharmacology (Curtis et al., 2025). The results are presented as the mean ± standard deviation (SD) or standard error of the mean (SEM). Graphs were prepared using Prism software (version 10) (GraphPad Software, USA). A Student's *t*-test (unpaired, two-tailed) was performed for comparisons between two groups, and one-way ANOVA was performed for comparisons among three or more groups, using Prism software. Post-hoc tests were run only if F achieved $P<0.05$ and there was no significant variance inhomogeneity.

2.14 | Nomenclature of targets and Ligands

Key protein targets and ligands in this article are hyperlinked to corresponding entries in the IUPHAR/BPS Guide to PHARMACOLOGY http://www.guidetopharmacology.org and are permanently archived in the Concise Guide to PHARMACOLOGY 2023/24 (Alexander, Cidlowski, Kelly, Mathie, Peters, Veale, Armstrong, Faccenda, Harding, Davies, Coons, et al., 2023; Alexander, Fabbro, Kelly, Mathie, Peters, Veale, Armstrong, Faccenda, Harding, Davies, Annett, et al., 2023; Alexander, Fabbro, Kelly, Mathie, Peters, Veale, Armstrong, Faccenda, Harding, Davies, Beuve, et al., 2023; Alexander, Kelly, Mathie, Peters, Veale, Armstrong, Buneman, Faccenda, Harding, Spedding, Cidlowski, et al., 2023).

3 | RESULTS

3.1 | N184 exhibited low cytotoxicity and enhanced $CD8^+$ T cell viability in vitro

A number of ASC derivatives were synthesised. Their core structure and side chain information are presented in Figure 1a, Table 2 and Supporting Information S1. The MO5 mouse melanoma cell line and mouse splenic T cells were cultured in the presence of 1, 5 or 10 μM of each compound for 3 days. Cytotoxicity was assessed and compared with ASC effects using a colorimetric assay (Figure 1b–d). ASC showed the greatest cytotoxic effect towards MO5, $CD4^+$ and $CD8^+$ T cells, at concentrations as low as 1 μM. N104, HK-11, N170, N174 and N200 exhibited moderate cytotoxicity at 1 μM, which increased in a concentration-dependent manner. Notably, N184 did not show any inhibition at 10 μM in these cells; however, it enhanced the $CD8^+$ T-cell survival rate (Figure 1d). N201, which shares a similar chemical structure with N184 (Figure S1, Table 2), exhibited a comparable cytotoxicity profile.

To determine the effect of N184 on T cell viability, $CD4^+$ and $CD8^+$ T cells were cultured in the presence of a wide range of concentrations of N184 for 4 to 6 days, and their viability was monitored by light microscopy. $CD4^+$ T cells treated with 10 μM N184 exhibited the highest cell viability compared with control cells at all time points, and 5 μM N184 enhanced viability on days 5 and 6 (Figure 1e); however, control $CD4^+$ T cells maintained 70% viability at day 6, represented only a ∼1.2-fold enhancement in viability.

In contrast, $CD8^+$ T cells cultured with 1, 5 and 10 μM N184 improved viability compared with control cells at all time points. Notably, 10 μM N184 markedly enhanced $CD8^+$ T cell viability, reaching approximately 5-fold higher compared with the control on day 6 (Figure 1f). Expression of anti-apoptotic proteins, Bcl-xL, Mcl-1 and phospho Bcl-2-associated death promoter (p-Bad), was upregulated in $CD8^+$ T cells treated with 10 μM N184 for 4 to 6 days (Figure 1g). Bcl2 upregulation was only slightly increased on days 4 and 5 of culture. Treatment with low concentrations of the

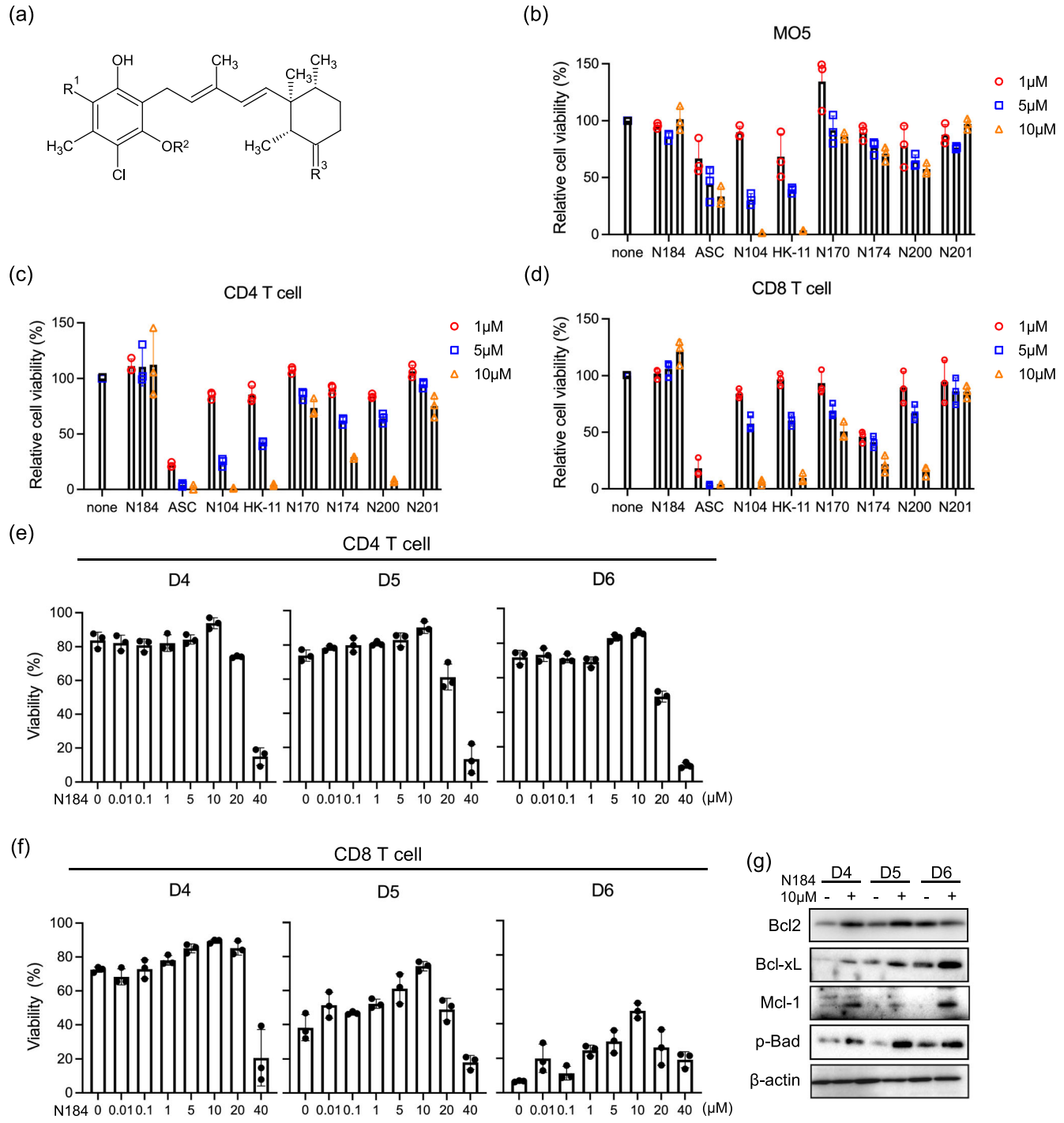

FIGURE 1 N184 enhances CD8$^+$ T cell survival through the inhibition of apoptosis. (a) Basic chemical structure of ASC and its derivatives. (b–d) Cells were cultured with ASC and its derivatives at 1, 5 or 10 μM for 2 days (MO5) (b) or 3 days (CD4$^+$ and CD8$^+$ T cells) (c,d). Cell viability was assessed using the CCK-8 assay. The data is presented as the mean ± SD. All experiments were repeated three times with consistent results (n = 3). (e,f) CD4$^+$ (e) and CD8$^+$ (f) T cells were cultured with N184 at 0.01 to 40 μM for 4–6 days. Viability was determined by counting live and dead cells under a microscope. The data is presented as the mean ± SD. All experiments were repeated three times with consistent results (n = 3). As n=3 for these experiments, statistical analysis was not carried out, and results should be regarded as preliminary. (g) Western blot analysis of anti-apoptotic protein expression in CD8$^+$ T cells cultured with 10 μM N184 for 4–6 days. This experiment was repeated three times with consistent results (n = 3).

ASC compound, which did not show cytotoxicity on day 3, and did not affect the viability of CD8$^+$ T cells on day 6, slightly enhanced CD4$^+$ T cell viability at especially 0.01 μM (Figure S2a). N201 enhanced CD8$^+$ T cell viability at 20 and 40 μM on day 6 of culture, whereas it did not increase the viability of CD4$^+$ T cells (Figure S2b).

TABLE 2 Chemical structure of ascochlorin and its derivatives.

Compound	R1	R2	R3	MW (g/mol)
Ascochlorin	-CHO	H	=O	409
N184	-CH=N-OMe	Me	$=N\text{-}OCH_2\text{-}CO_2H$	525
N104	-CHO	CH_2F	=O	441
HK-11	$-CH=N\text{-}CH_2C=O\text{-}NH_2$	Me	=O	508
N170	-CH=N-OMe	Me	=N-OMe	481
N174	-CH=N-OMe	Me	=N-OH	467
N200	-CHO	CH_2F	$=N\text{-}OCH_2\text{-}CO_2H$	514
N201	-CH=N-OH	CH_2F	$=N\text{-}OCH_2\text{-}CO_2H$	529

3.2 | N184 exerted an antitumour effect, depending on $CD8^+$ T cells in vivo

Based on the results of in vitro experiments, we examined the antitumour effect of N184 in vivo. N184 was orally administered to MO5-bearing mice at doses prepared by three-fold serial dilutions from an initial concentration of 100 mg kg^{-1}. Significant inhibition of tumour development was observed in a dose-dependent manner, with the most pronounced suppression observed at 100 mg kg^{-1} (Figures 2a and S3a), and the effect of N184 was exerted most at day 7 compared to treatments from day 10 or 13 after tumour inoculation (Figures 2b and S3b). The antitumour effect of N184 was completely abrogated in immunodeficient mice (SCID) (Figures 2c and S3c). As expected, the in vivo depletion of $CD8^+$ T cells completely abolished the antitumour response (Figures 2d and S3d), confirming that $CD8^+$ T cells are essential for N184-induced tumour suppression. In addition to MO5, N184 also suppressed the growth of MethA, a fibrosarcoma cell and CT26, a colon cancer cell (Figure S3e).

$CD8^+$ tumour infiltrating lymphocytes ($CD8^+$ TILs) were analysed by flow cytometry (Figure S4). The capacity to produce triple cytokines (IL-2, IFNγ, TNFα) was higher with N184 on day 13 (Figure 2e). To evaluate cytotoxicity of $CD8^+$ TILs, surface expression of CD107a was detected but there was no change (Figure 2f). The central memory (T_{CM}; $CD44^+CD62L^+$), the effector memory (T_{EM}; $CD44^+CD62L^-$), and the stem cell memory (T_{SCM}; $CD44^-CD62L^+$) populations were compared. T_{EM} was found to be dominant over T_{CM} in N184-treated group (Figure 2g). And T_{SCM} was not detected. We next investigated the Bcl2 expression in the context of T_{CM}/T_{EM} classification. $CD8^+$ TILs of mice treated with N184 were revealed to express higher Bcl2 in both T_{CM} and T_{EM} than those of control mice (Figure 2h). The high expression of Bcl2 is expected to suppress cell death of $CD8^+$ TILs, thereby extending their lifespan.

3.3 | N184 promotes the expression of IL-2 and IL-9 mRNAs and contributes to T cell viability

We determined whether the enhanced viability of $CD8^+$ T cells induced by N184 was mediated by soluble factors, such as cytokines, secreted into the culture supernatant by N184-treated $CD8^+$ T cells. For this purpose, on day 3 of culture, the 90% $CD8^+$ T cell culture medium containing N184 [N184 (+) sup] was replaced with 90% $CD8^+$ T cell culture medium without N184 [N184 (−) sup]. The cells were cultured for an additional 3 days to compare viability (Figure 3a). As a result, the viability of the N184(−) cells replaced with N184 (+) sup was markedly increased. In contrast, the viability of N184 (+) cells replaced with N184 (−) sup was decreased (Figure 3b). The results indicated that the N184-dependent increased viability of $CD8^+$ T cells was mediated by soluble factors, such as cytokines, from N184-treated $CD8^+$ T cells in an autocrine-dependent manner.

Cytokines involved in the proliferation and survival of T cells include IL-2, IL-4, IL-7, IL-9 and IL-15. Their receptors have a common γ chain. Therefore, we examined the production of these cytokines by $CD8^+$ T cells cultured for 3 to 5 days following TCR stimulation by qPCR. $CD8^+$ T cells were stimulated with or without PMA/ionomycin for 3 h before RNA extraction. Throughout the 3- to 5-day cultures, the expression of *Il2*, *Il9* and *Il15* was increased by N184, even without PMA/ionomycin stimulation (Figure 3c,e,f). However, *Il2* expression on day 3 of culture with PMA/ionomycin was slightly decreased by N184 (Figure 3c). The expression of *Il7* was very low to negligible under the conditions tested (Figure 3d). *Il4* expression was not detected. *Il15* expression was lower compared with that of *Il2* and *Il9*, and there was no enhancement following PMA/ionomycin stimulation (Figure 3f).

To assess the functional relevance of these cytokines, the viability test was performed with or without neutralising antibodies against the cytokines. N184(+) sup on day 3 of culture was incubated with the indicated antibodies for 30 min and replaced with N184(−) sup. As a result, either antibody alone against IL-2 or IL-9 partially blocked the N184-mediated viability-enhancing effect, whereas treatment with both antibodies completely blocked the effect (Figure 3g). Next, neutralising antibodies to IL-2, IL-9 and IL-15 were directly added to the culture wells on day 3 as indicated, and viability was assessed after an additional 3-day incubation. The N184-dependent viability-enhancing effect was partially ameliorated by single treatment with anti-IL-2 or anti-IL-9 mAb, whereas it was completely abrogated by treatment with both antibodies (Figure 3h). Single treatment with anti-IL-15 mAb did not show any blocking effect, moreover, treatment with anti-IL-2, anti-IL-9 mAb and anti-IL-15 mAb in combination did not enhance the effect of the dual treatment with anti-IL-2 and anti-IL-9 mAb (Figure 3h). This indicated that the effect of IL-15 was negligible. Control $CD8^+$ T cells exhibited slight sensitivity to anti-IL-2

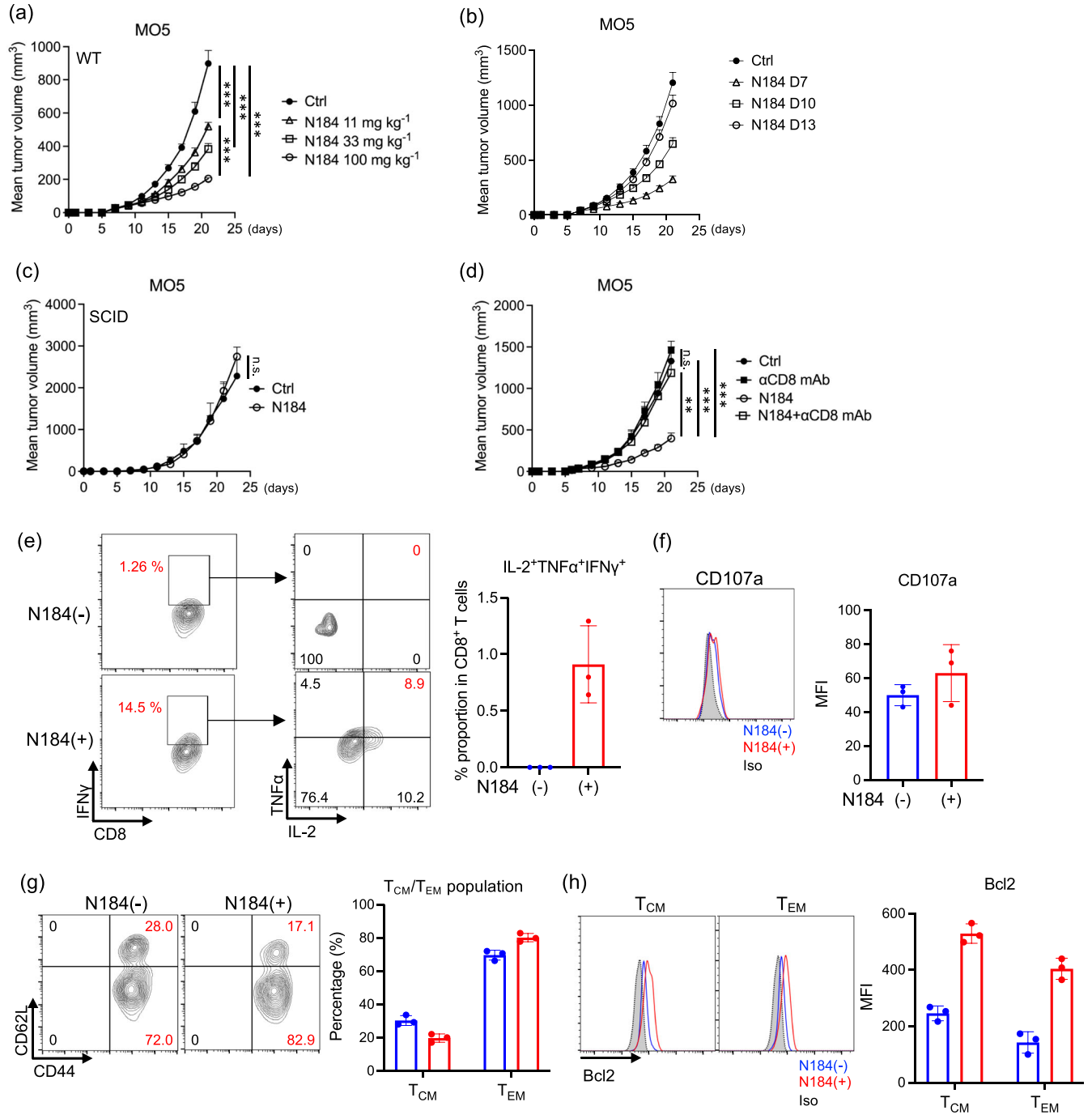

FIGURE 2 N184 suppressed tumour growth in vivo in a $CD8^+$ T cell-dependent manner. (a) B6 mice were intradermally inoculated with 2.0×10^5 MO5 cells and received N184 at doses of 11, 33 and 100 mg kg^{-1} or vehicle control (Ctrl) every other day beginning on day 7 post-inoculation Tumour diameter was measured every other day. (n = 5 per group). (b) MO5 inoculated B6 mice received 100 mg kg^{-1} N184 from day 7, 10 or 13 post-inoculation (n = 4 per group). (c) SCID mice inoculated with MO5 cells received 100 mg kg^{-1} N184 from day 7 (n = 5 per group). (d) MO5 inoculated B6 mice received N184 from day 7 and anti-CD8 mAb was injected intraperitoneally on days 6 and 10 (n = 4 for αCD8 mAb group, n = 5 for other groups). Tumour growth was monitored until day 21 (a,b) and day 23 (c,d). Tumour volume is presented as the mean ± SEM. (e) On day 13, $CD8^+$ TILs were recovered from MO5 tumour masses and pooled from 5 mice per group. After stimulation with PMA and ionomycin for 6 h, cytokine production was monitored. The populations of cytokine producing $CD8^+$ TILs on day 13 is shown. Gated populations for $CD8^+IFN\gamma^+$ was further analysed for their production of $TNF\alpha^+IL\text{-}2^+$ and triple cytokine produce proportion was calculated. (f–h) $CD8^+$ TILs were recovered on day 13 and examined CD107a (f) and CD44, CD62L (g) and Bcl2 (h). Results are representative of three independent experiments, respectively (n = 3). The data is presented as the mean ± SD. Statistical significance was determined by a two-tailed Student's test (c) or one-way ANOVA (a, d): $^{**}P < 0.01$, $^{***}P < 0.001$.

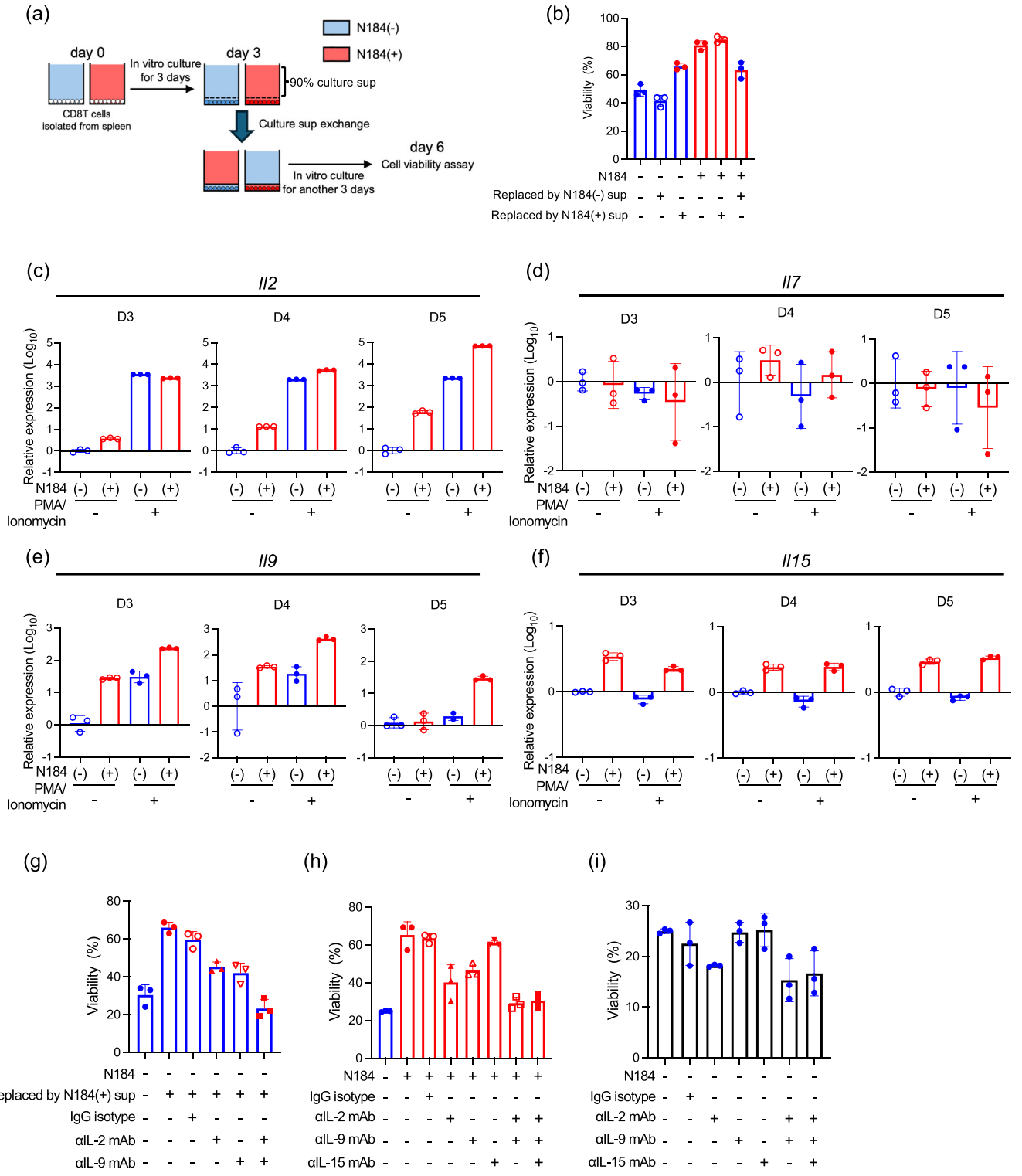

FIGURE 3 N184 prolonged $CD8^+$ T cell viability through production of IL-2 and IL-9. (a) Experimental protocol: $CD8^+$ T cells were cultured with 10 μM N184 for 3 days. Next, 180 μl of culture supernatant out of a total 200 μl was either exchanged between the N184(−) and N184(+) groups or added back to the original wells as a sham control. Cell viability was assessed on day 6 (b). (c–f) $CD8^+$ T cells were cultured with 10 μM N184 for 3–5 days. Following stimulation by PMA and ionomycin for 3 h, total RNA was extracted to measure *Il2* (c), *Il7* (d), *Il9* (e) and *Il15* (f) detection by qPCR. (g) Culture supernatant was supplemented with 10 μg mL^{-1} of anti-IL-2 or IL-9 Abs and exchanged between the N184(−) and N184(+) groups on day 3, and cell viability was assessed. (h,i) Antibodies against IL-2, IL-9 and IL-15 (10 μg mL^{-1}) were directly added to N184 (+) (h) or N184(−) (i) culture groups on day 3, and cell viability was evaluated. Data are presented as the mean ± SD. All experiments were independently repeated with consistent results (n = 3). As n=3 for these experiments, statistical analysis was not carried out, and results should be regarded as preliminary.

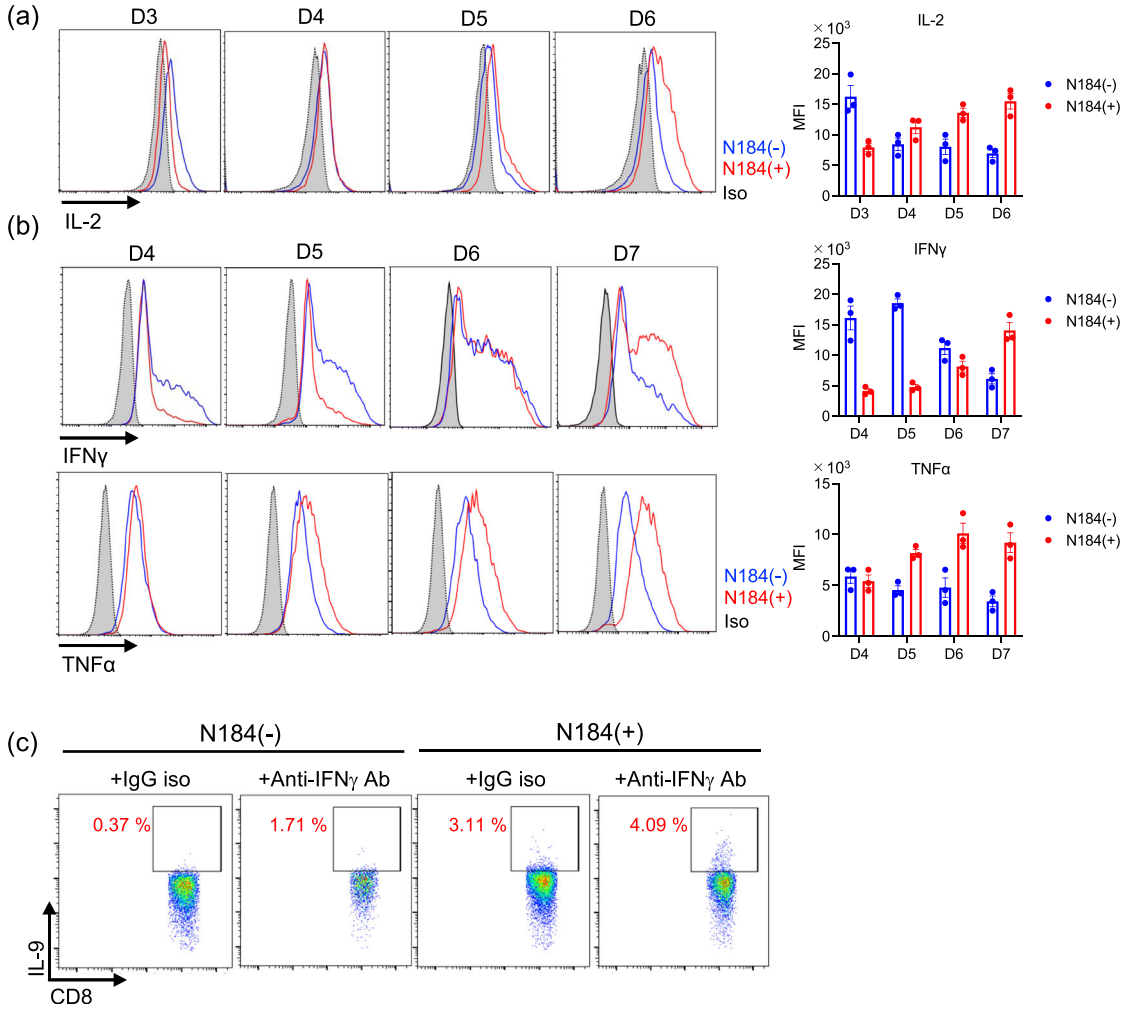

FIGURE 4 N184-treated CD8$^+$ T cells displayed a cytokine production profile resembling that observed during differentiation of the Tc9 subset. (a, b) CD8$^+$ T cells were cultured with 10 μM N184 for 3–7 days. Cells were stimulated with PMA and ionomycin for 6 h, and IL-2 (a), IFNγ and TNFα (b) were measured. Representative histograms (left panels) and quantification of mean fluorescence intensity (MFI, right panels). Data are presented as the mean ± SEM (n = 3). As n=3 for these experiments, statistical analysis was not carried out, and results should be regarded as preliminary. (c) CD8$^+$ T cells were cultured with 10 μM N184 in medium containing 10 μg mL^{-1} anti-IFNγ mAb or isotype control for 4 days. IL-9 expression was assessed following incubation in FCS-free medium for 6 h, used as a PMA/ionomycin nonstimulated control. This experiment was repeated independently with consistent results (n = 3).

mAb treatment, whereas anti-IL-9 and anti-IL-15 antibodies had no effect (Figure 3i).

Because 40 μM N201 also enhanced CD8$^+$ T cell viability, we examined *Il9* expression in N201-treated CD8$^+$ T cells. We found that N201 also induced *Il9* expression (Figure S5). Since N184 was available in greater quantities than N201, subsequent experiments were performed with N184.

3.4 | N184 induced a noncanonical cytokine expression pattern in CD8$^+$ T cells compared with the Tc1 subset

Flow cytometry analysis was performed to confirm cytokine production at the protein level (Figure 4). IL-2 production was initially suppressed on day 3 and subsequently increased by day 5 in N184-treated cells (Figure 4a), whereas the control cells (Tc1 subset) progressively lost IL-2 production capacity, which is consistent with the qPCR results (Figure 3c). IFNγ and TNFα were used to evaluate the ability of CD8$^+$ T cells to produce multiple cytokines, which is referred to as multifunctionality (Eikawa et al., 2015) (Figure 4b). IFNγ production was markedly suppressed on days 4 and 5 in N184-treated cells, compared to that in Tc1 subset. Based on the qPCR results, this suppression was primarily due to transcriptional repression (Figure S6a); however, production was gradually restored by day 7 and surpassed the IFNγ production level of the control cells. In addition, we examined cytotoxicity of CD8$^+$ T cells on day 7. Unlike IFNγ expression, N184-treated cells showed a significant decrease in **granzyme B** expression while **perforin** expression remained largely unchanged (Figure S6b), and cell surface CD107a expression was also slightly reduced (Figure S6c), indicating the

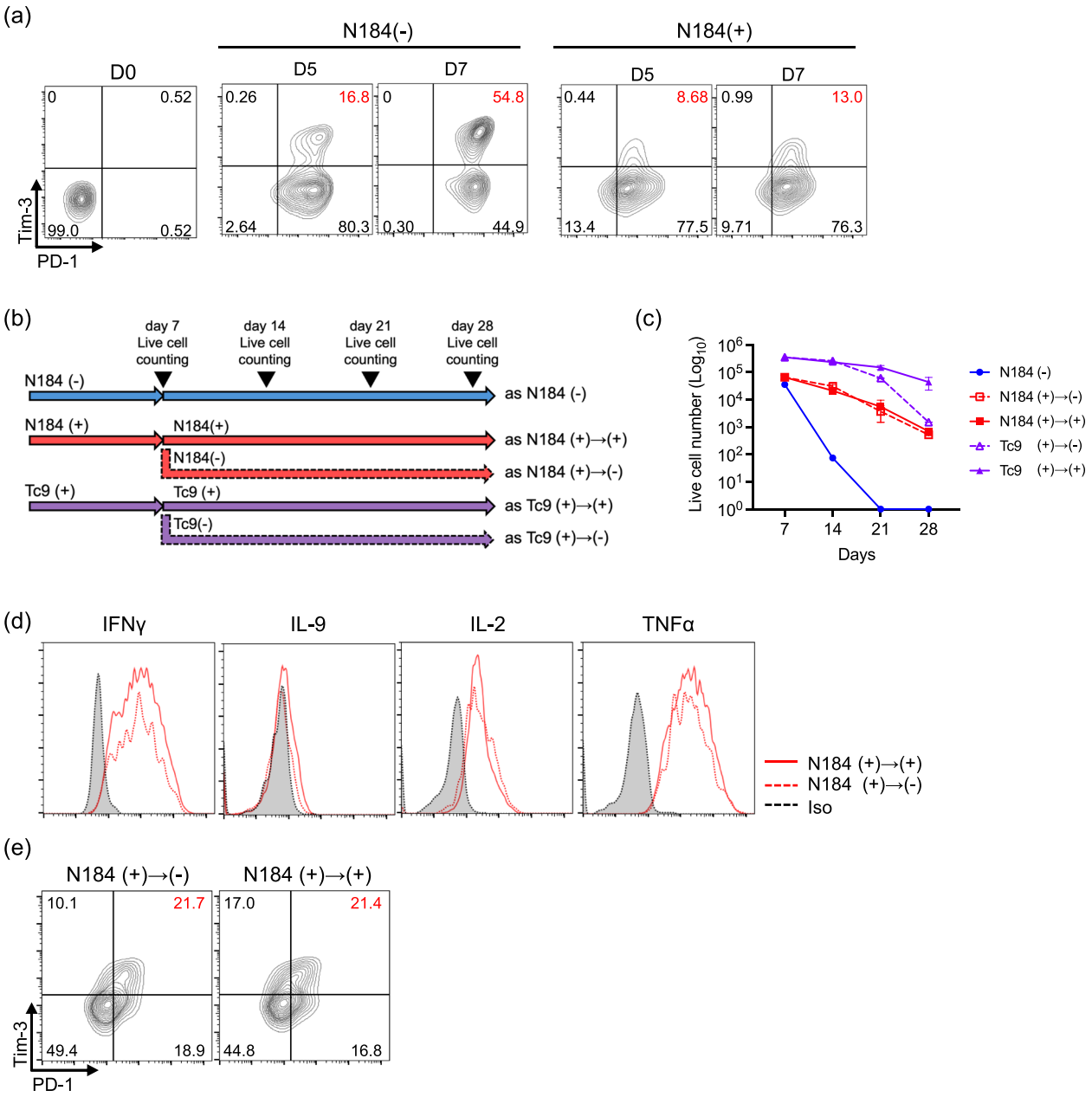

FIGURE 5 The first 7 days of coculture with N184 maintained the viability, cytokine production and exhaustion status of $CD8^+$ T cells for subsequent cultures. (a) $CD8^+$ T cells were cultured with 10 μM N184 for 5 or 7 days. Exhaustion markers, PD-1 and TIM3, were assessed by flow cytometry. Isolated splenic $CD8^+$ T cells were stained as the day 0 control (D0). This experiment was performed three times with consistent results (n = 3). (b) Schematic of the experimental procedure: $CD8^+$ T cells were cultured with 10 μM N184 or Tc9-polarised medium for 7 days. Next, the cells were divided into two groups, N184(−) or N184(+) /Tc9(−) or Tc9(+) and cultured with anti-CD3 and CD28 mAbs for an additional 7–21 days. Live cell numbers were monitored weekly until day 28 (c). Data are presented as the mean ± SEM (n = 3). Cytokine production capacity (d) and exhaustion marker expression (e) of N184-treated cells were assessed on day 14. All experiment was performed three times with consistent results (n = 3). As n=3 for these experiments, statistical analysis was not carried out, and results should be regarded as preliminary.

possibility of decreased cytotoxicity. The reduced cytotoxicity in N184-treated cells is critically different from the character of Tc1 subset.

In contrast to IFNγ, TNFα secretion was persistently elevated in N184-treated cells on day 5 and beyond. IL-9 protein levels were slightly increased in N184-treated $CD8^+$ T cells (Figure 4c). Because IL-9 production is suppressed by IFNγ (Murugaiyan et al., 2012), we determined whether neutralising Abs to IFNγ increases IL-9 production. Indeed, both the mRNA and protein levels were upregulated following the blockade of IFNγ (Figures 4c and S6d), and N184-treated T cells with anti-IFNγ Ab showed the highest number of IL-9^+ $CD8^+$ T cells (Figure 4c). These cytokine expression phenotypes resemble the differentiation process from naive $CD8^+$ T cells to the Tc9 subset (Lu, Wang, & Yi, 2014).

We therefore compared cytokine production between N184-treated $CD8^+$ T cells and Tc9 cells on days 3 and 7. Tc9 cells produced increased levels of IL-9 on day 7 (Figure S6e). IFN-γ production was inhibited in both N184-treated $CD8^+$ T cells and Tc9 cells on day 3 (Figure S6f) but recovered on day 7 (Figure S6g). TNF-α expression was higher in Tc9 cells than in N184-treated $CD8^+$ T cells. However, IL-2 expression was higher in N184-treated cells than Tc9 cells (Figure S6g).

3.5 | The first 7 days of coculture with N184 maintained viability, cytokine production and improved $CD8^+$ T cell exhaustion even without N184 in subsequent cultures

Long-term T-cell stimulation results in the expression of exhaustion markers, such as Programmed cell death protein 1 (**PD-1**) and T-cell immunoglobulin and mucin domain 3 (**TIM3**), followed by T-cell dysfunction (Wherry, 2011). We therefore determined the effect of N184 on the expression of exhaustion markers. The terminally exhausted PD-1^+ $TIM3^+$ populations were markedly reduced on days 5 and 7 in N184-treated $CD8^+$ T cells compared with those of the untreated cells (Figure 5a). In addition, we examined memory phenotype, but there was no difference between control and N184-treated cells, moreover, we could not detect a T_{SCM} population (Figure S7a).

Next, we determined whether the improved cell viability and decreased exhaustion markers observed in N184-treated on day 7 culture were maintained over longer culture periods and whether constant contact with N184 was required to achieve this phenomenon. We also investigated differences between N184-treated and Tc9-polarised cells (Figure 5b). The control cells failed to survive secondary TCR restimulation on day 7, with viable cell numbers markedly lower compared with those of the N184-treated cells on day 14, and they were completely dead by day 21. In contrast, 7-day N184-treated cells remained viable throughout the culture period (Figure 5c). Tc9 polarised cells displayed 10-fold higher cell numbers than N184-treated cells by day 14, but required continued treatment with polarising medium to maintain their viability from day 21 onwards (Figure 5c). Cytokine production (Figure 5d) and reduced exhaustion marker levels (Figure 5e) in N184-treated $CD8^+$ T cells were maintained, even after the second week of culture. In the presence or absence of N184, the second culture was not associated with survival (Figure 5c), cytokine production (Figure 5d) or exhaustion status (Figure 5e). In contrast to N184, the PD-$1^+$$TIM3^+$ population of Tc9 cells on day 14 was clearly higher, and the cells cultured with nonpolarised medium showed a higher state of exhaustion than cells cultured in polarised medium from day 7 (Figure S7b).

3.6 | N184 is essential during early $CD8^+$ T-cell differentiation for improving cell survival and exhaustion, while dispensable for enhancing cytokine production

To determine whether N184 treatment during the initial phase of TCR stimulation is required for the differentiation of $CD8^+$ T cells with a Tc9-like character, $CD8^+$ T cells were incubated with N184 at various time points (Figure 6a). Cell viability on day 6 was affected by the timing of N184 treatment (Figure 6b). Thus, the administration of N184 within the first 24 h was necessary to prolong cell viability. N184 treatment within the first 24 h was required for the maximum reduction of terminally exhausted PD-$1^+$$TIM3^+$ cells, although all N184-treated groups showed lower expression of exhaustion markers compared with the control cells (Figure 6c). In contrast, the production of IFNγ, IL-2 and TNFα remained unchanged across all treatment times from days 0 to 3 (Figure 6d). Notably, IL-9 production was enhanced by the presence of N184 during TCR stimulation, but the effect gradually disappeared after 24 h or longer (Figure 6e).

3.7 | The N184-mediated antitumour effect depended entirely on IFNγ and partially on IL-9 in vivo

Because N184 promoted the expression of IFNγ and IL-9 to varying degrees in vitro, either cytokine may contribute to the antitumour effect of N184. To clarify the IFNγ requirement, two melanoma cell lines, B16 fucci as a control and B16 fucci-δIC, were established. The latter overexpresses a deletion mutant of the cytoplasmic domain of the IFNγ receptor, which abrogates signal transduction upon IFNγ binding (Matsushita et al., 2015). Treatment with N184 suppressed tumour growth in B16 fucci-bearing mice, whereas it did not affect tumour growth in B16 fucci-δIC-bearing mice. This indicated that IFNγ signalling in tumour cells is essential (Figures 7a,b and S8a,b). Injection of anti-IL-9 mAb in MO5-bearing mice partially decreased the antitumour effect of N184 (Figure 7c and S8c), whereas it did not affect the antitumour effect of metformin (Figures 7d and S8d). Of note, we and others previously reported an immune-mediated antitumour response with metformin (Eikawa et al., 2015; Finisguerra et al., 2023; Nishida et al., 2021; Zhang et al., 2020), suggesting that IL-9 specifically contributed to the efficacy of N184, but not metformin. These results demonstrated that the antitumour effect of N184 requires IFNγR signalling and, to a lesser extent, IL-9.

3.8 | In vitro modelling of IL-9 neutralisation revealed selective effects on $CD8^+$ T cell viability

To determine the effect of IL-9 blockade on $CD8^+$ T cells in vivo (Figure 7c), $CD8^+$ T cells were cultured in vitro with 10 μM N184 and 10 μg mL^{-1} anti-IL-9 mAb from day 0. Cell viability was partially decreased by IL-9 blockade (Figure 8a), which was consistent with previous results (Figure 3g,h). In contrast, no changes were observed in the expression of exhaustion markers on day 7 (Figure 8b) or the production of cytokines on days 3 and 7 (Figure 8c). This indicated the selective contribution of IL-9 to the enhanced cell survival of $CD8^+$ T cells.

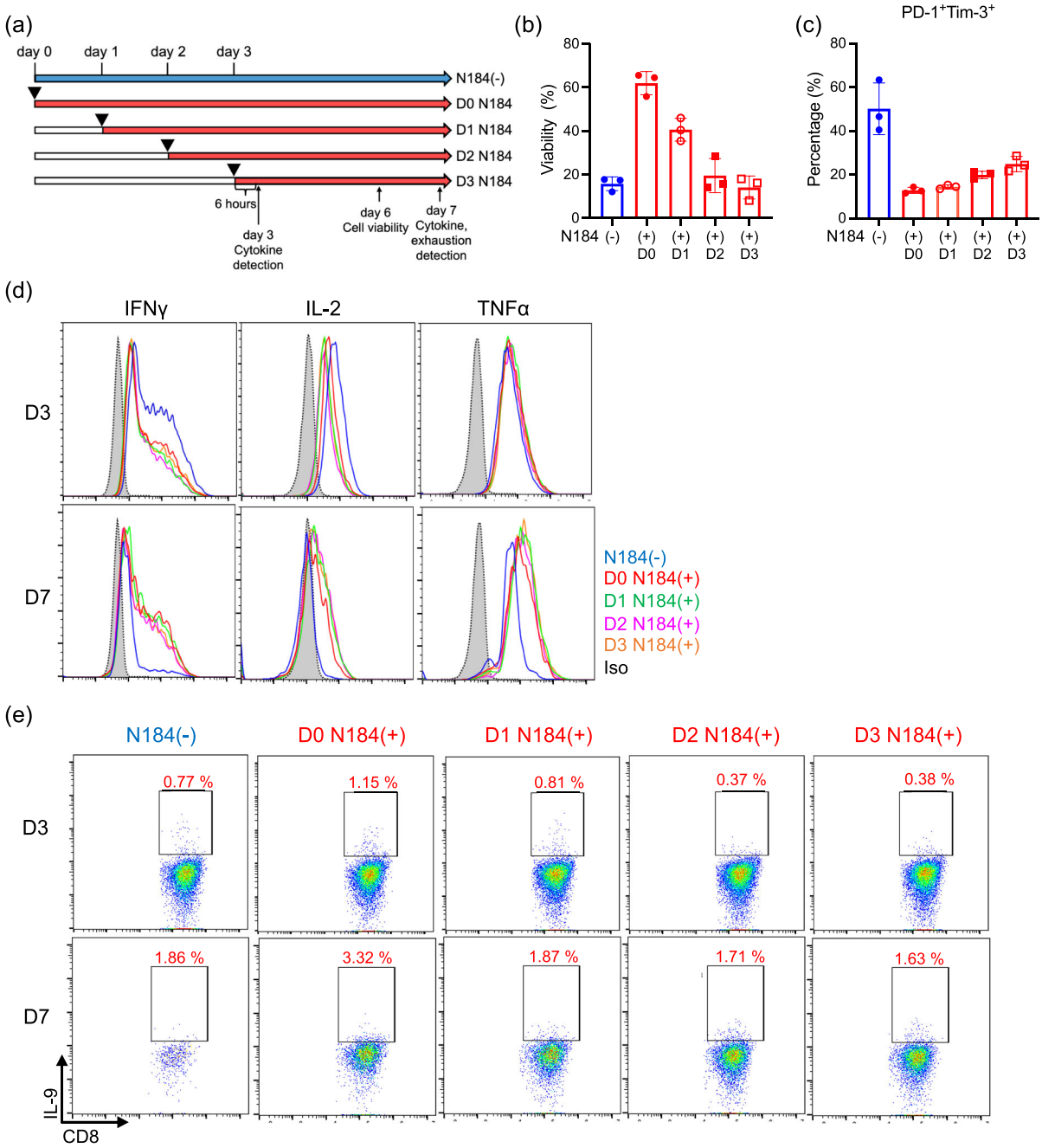

FIGURE 6 Effects of N184 treatment timing on CD8$^+$ T cell viability and function. (a) Experimental procedure: CD8$^+$ T cells were initially cultured with or without 10 μM N184. N184 was added to the N184(−) culture wells at 24, 48 and 72 h after culture initiation. Cell viability was assessed on day 6 (b). Exhaustion marker expression on day 7 (c) and cytokine production on days 3 and 7 (d,e) were evaluated by flow cytometry. The data are presented as the mean ± SD. All experiments were performed three times with consistent results (n = 3). As n=3 for these experiments, statistical analysis was not carried out, and results should be regarded as preliminary.

4 | DISCUSSION

In this study, the ASC derivatives, N184 and N201, were 10-fold less toxic to mouse T cells compared with ASC. N184 and N201 were not only less cytotoxic, but they also enhanced the survival rate of proliferating CD8$^+$ T cells following TCR stimulation compared with those cultured in the absence of the compounds. Peak activity was observed at 10 and 40 μM, respectively. No such survival benefit was observed in CD4 T cells. N184 and N201 share –CH=N–O in their R1 side chain and =N–OCH_2–COOH in their R3 side chain. Interestingly, both induced low but reproducible amounts of IL-9 production from TCR-stimulated CD8$^+$ T cells. Thus, the shared side chain structures found in the two compounds may be involved in IL-9 production from CD8$^+$ T cells.

The survival-prolonging effect of N184 was observed at a lower concentration of 10 μM compared with N201 at 40 μM. Treatment

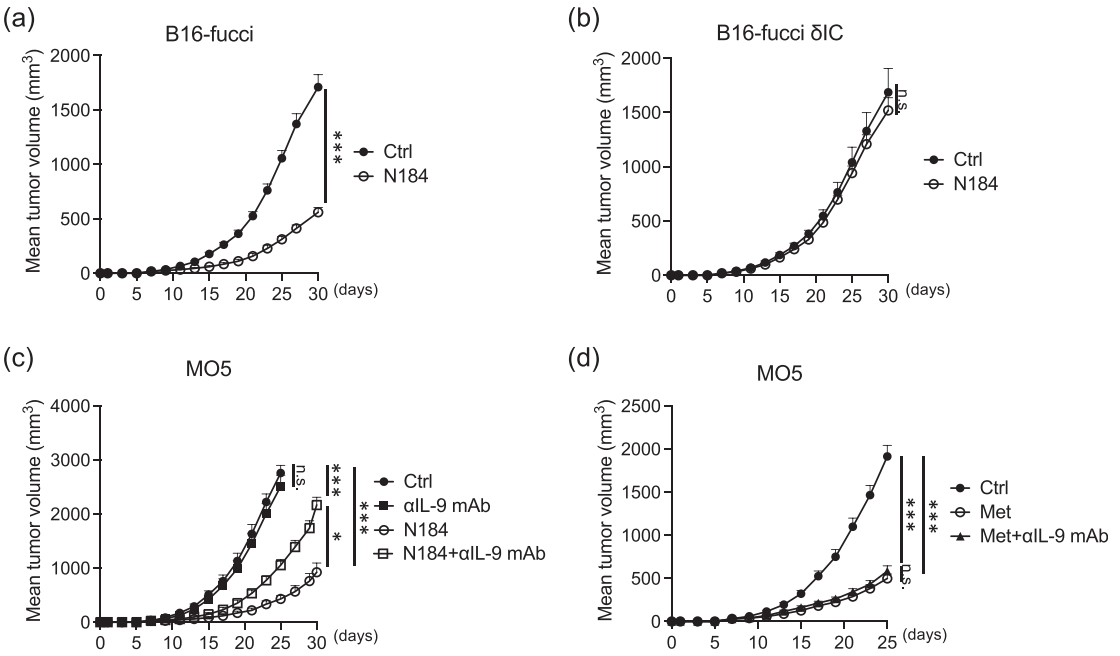

FIGURE 7 Requirement of IFNγ and IL-9 in the N184-mediated antitumour effect. (a,b) B6 mice inoculated with 2.0×10^5 B16-fucci or B16-fucci δIC cells were treated with 100 mg kg^{-1} N184 every other day from day 7, and tumour growth was monitored until day 30. (c,d) MO5-injected B6 mice received N184 (c), or metformin through free drinking water at 5 mg ml^{-1} (d) from day 7. Anti-IL-9 mAb (300 μg per animal) was administered every 3 days concurrently with N184 or metformin treatment. Tumour growth was monitored until day 25 for the control and αIL-9 mAb groups or until day 30 for N184 and N184 + αIL-9 mAb (c) and until day 25 (d). All data are presented as the mean ± SEM (n = 5 per group). Statistical significance was determined by a two-tailed Student's test (a, b) or one-way ANOVA (c, d) at the experimental endpoint or on day 25 (c): $^{**}P < 0.01$, $^{***}P < 0.001$.

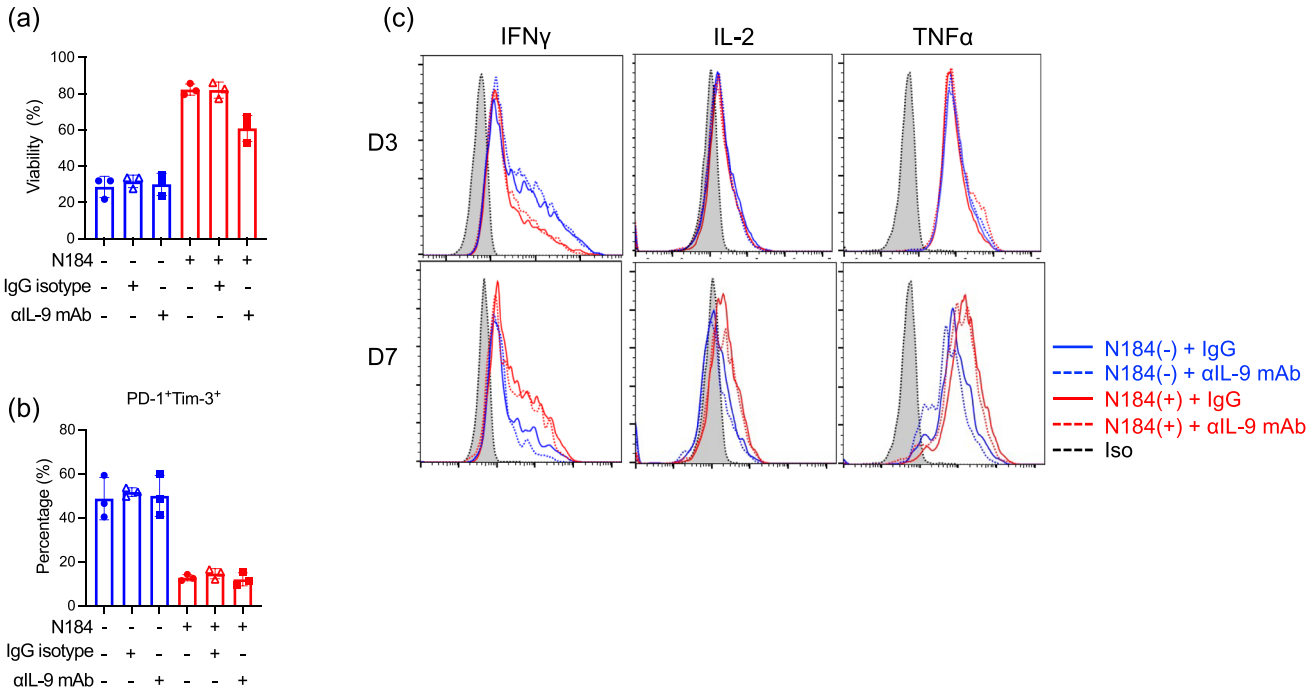

FIGURE 8 Anti-IL-9 mAb treatment partially abrogated the enhanced viability of N184-treated $CD8^+$ T cells without affecting cytokine production or exhaustion marker expression. $CD8^+$ T cells were cultured with 10 μM N184 in the presence or absence of 10 μg mL^{-1} anti-IL-9 mAb for 7 days. Cell viability was assessed on day 6 (a). Exhaustion marker expression on day 7 (b) and cytokine production on days 3 and 7 (c) were evaluated by flow cytometry. Data are presented as the mean ± SD. All experiments were performed three times with consistent results (n = 3). As n=3 for these experiments, statistical analysis was not carried out, and results should be regarded as preliminary.

with 10 μM N184 not only enhanced the survival rate, but also improved cytokine production and immune exhaustion of TCR-stimulated $CD8^+$ T cells during the late stages of culture (day 7) compared with those of the untreated cells. These three effects were not all dependent on IL-9, because only the survival-enhancing effect was blocked by an anti-IL-9 Ab, whereas the effects on cytokine production and exhaustion were not. The survival-extending effect was observed when N184 was administered within 24 h following TCR stimulation. Furthermore, the high survival rate was maintained, even when N184 was removed during the second week of culture. This suggests that N184 is involved in determining the early differentiation of $CD8^+$ T cells.

Suppression of IFNγ production up to the third or fourth day of N184 culture was also observed in Tc9 cells, which were induced to differentiate in an IL-4- and TGFβ-dependent manner (Lu, Hong, et al., 2014). IFNγ production was reported to remain suppressed even during the late stage of Tc9 culture (Visekruna et al., 2013). However, in our culture system, the production of not only IFNγ but also cytokines, such as TNFα and IL-2, were increased in both N184-induced $CD8^+$ T cells and Tc9 subset on day 7 of culture compared with those of untreated $CD8^+$ T cells. Importantly, IFNγ and TNFα production in Tc9 cells tended to be higher than in N184-treated cells, whereas IL-2 production was lower. This difference in cytokine expression patterns may suggest that N184-treated cells represent a distinct cell population from Tc9. The apparent difference in the degree of exhaustion between Tc9 and N184-treated cells also supports this possibility.

Oral administration of N184 reduced tumour growth in WT mice, but not in immunodeficient SCID mice, and the effect was dependent on $CD8^+$ T cells and IFNγ R signalling in tumour cells. The results indicate that the N184-induced antitumour effect is mediated by the immune system, and the effector molecule is IFNγ produced by $CD8^+$ T cells. The lack of an increase in CD107a upon N184 treatment may support that IFNγ is primarily an important effector mechanism for the antitumour effect of N184. IFNγ is known to induce cell cycle arrest and apoptosis in cancer cells, which possibly release tumour antigens that can be presented by dendritic cells to prime and activate tumour specific $CD8^+$ T cells in vivo. This immune-related feature is unique to N184, because the reported antitumour effects of the parent compound ASC and/or its other derivatives have been attributed to direct inhibitory effects on tumour cells (Cho et al., 2018; Dai et al., 2015; Gan et al., 2025; Hong et al., 2005; Sakaguchi et al., 2005; Seok et al., 2018). The administration of anti-IL-9 Ab on day 7 post-tumour challenge showed only partial inhibition of the N184-mediated antitumour effect. Neutralisation of IL-9 in vivo may cancel the N184-mediated IL-9-dependent survival-prolonging effect for $CD8^+$ T cells, but not the N184-mediated cytokine-enhancing effect. Therefore, the cytokine-enhancing effect may contribute to the partial antitumour effect with IL-9 blockade. This may be reasonable based on the results of in vitro experiments showing that anti-IL-9 Ab blocks only the survival-prolonging effect and not the effects on cytokine production and exhaustion.

The cell survival-enhancing effect was only modest in $CD4^+$ T cells by N184. Most experiments were focused on the analysis of $CD8^+$ T cells in the present study; however, $CD4^+$ T cells, including $FoxP3^+$ regulatory T cells (Tregs), are likely involved in the N184-mediated antitumour effect, whereas dissection of $CD4^+$ T cells in vitro and in vivo will be necessary in future studies. Likewise, the effect of N184 on other cell populations comprising the tumour microenvironment (TME), such as dendritic cells (DCs), tumour-associated macrophages, myeloid-derived suppressor cells, cancer-associated fibroblasts and tumour vessels, will be necessary to determine the effect of N184 on the TME.

In conclusion, we successfully identified two ASC analogues, N184 and N201, which prolong the survival of $CD8^+$ T cells following TCR stimulation. These two compounds stimulate $CD8^+$ T cells to produce IL-9, albeit in small amounts, which may induce a survival-prolonging effect. Of the two compounds, N184, which was considered less cytotoxic, shrinks solid tumours when administered orally in vivo. This was found due to the activation of immune $CD8^+$ T cells. $CD8^+$ T cells induced to differentiate by N184 not only have an extended lifespan, but also significantly increase the production of IFNγ, IL-2 and TNFα, with reduced exhaustion markers, which suggests that they may represent a new cell population distinct from the previously reported Tc9 subset. This unique feature of N184 may be applicable to tumour-specific T-cell adoptive therapy and chimeric antigen receptor (CAR)-T cell therapy by coculturing with TCR stimulation. Although the potential clinical application is compelling, the effects of N184 on the IL-9 production and differentiation of human $CD8^+$ T cells must be investigated. Another important issue to be investigated is the extent to which N184 has an inhibitory effect on cancer metastasis, the cause of death of more than 90% of cancer patients. Further analysis is warranted to gain a comprehensive understanding of the effect of N184 on immunity and tumour growth prevention.

AUTHOR CONTRIBUTIONS

Natsumi Imano and Mikako Nishida performed experiments and wrote the paper. Miho Tokumasu performed data analysis. Weiyang Zhao performed experiments. Nahoko Yamashita maintained the mice to be used for the experiments. Heiichiro Udono designed the study and wrote the paper. All authors contributed to the final version of the manuscript.

ACKNOWLEDGEMENTS

We thank the Central Research Laboratory, Okayama University Medical School.

We also thank for Dr. Hoshino in NRL Pharma, Inc. who kindly provided us ASC and its derivatives. This study was supported by grants to H.U. from Japan Society for the Promotion of Science (JSPS) Grants-in-Aid for Scientific Research (KAKENHI) (Grant Numbers 18H04033, 17K19598, and 24K02326) and by JST SPRING, Japan Grant Number JPMJSP2126. The graphical abstract was created with Biorender.com.

CONFLICT OF INTEREST STATEMENT

The authors have no competing interest.

DATA AVAILABILITY STATEMENT

The data that support the findings of this study are available from the corresponding author upon reasonable request. Some data may not be made available because of privacy or ethical restrictions.

DECLARATION OF TRANSPARENCY AND SCIENTIFIC RIGOUR

This declaration acknowledges that this paper complies with the principles of transparent reporting and scientific rigour for preclinical research as outlined in the BJP guidelines on Design and Analysis, Immunoblotting and Immunochemistry and Animal Experimentation, as well as the principles recommended by funding agencies, publishers and other organisations involved in supporting research.

ORCID

Natsumi Imano https://orcid.org/0009-0007-1342-4813
Mikako Nishida https://orcid.org/0000-0003-1538-7263
Miho Tokumasu https://orcid.org/0000-0001-7654-3149
Heiichiro Udono https://orcid.org/0000-0002-9407-2296

REFERENCES

Alexander, S. P. H., Cidlowski, J. A., Kelly, E., Mathie, A. A., Peters, J. A., Veale, E. L., Armstrong, J. F., Faccenda, E., Harding, S. D., Davies, J. A., Coons, L., Fuller, P. J., Korach, K. S., & Young, M. J. (2023). The Concise Guide to PHARMACOLOGY 2023/24: Nuclear hormone receptors. *British Journal of Pharmacology*, *180*(S2), S223–S240. https://doi.org/10.1111/bph.16179

Alexander, S. P. H., Fabbro, D., Kelly, E., Mathie, A. A., Peters, J. A., Veale, E. L., Armstrong, J. F., Faccenda, E., Harding, S. D., Davies, J. A., Annett, S., Boison, D., Burns, K. E., Dessauer, C., Gertsch, J., Helsby, N. A., Izzo, A. A., Ostrom, R., Papapetropoulos, A., … Wong, S. S. (2023). The concise guide to PHARMACOLOGY 2023/24: Enzymes. *British Journal of Pharmacology*, *180*, S289–S373. https://doi.org/10.1111/bph.16181

Alexander, S. P. H., Fabbro, D., Kelly, E., Mathie, A. A., Peters, J. A., Veale, E. L., Armstrong, J. F., Faccenda, E., Harding, S. D., Davies, J. A., Beuve, A., Brouckaert, P., Bryant, C., Burnett, J. C., Farndale, R. W., Friebe, A., Garthwaite, J., Hobbs, A. J., Jarvis, G. E., … Waldman, S. A. (2023). The Concise Guide to PHARMACOLOGY 2023/24: Catalytic receptors. *British Journal of Pharmacology*, *180*, S241–S288. https://doi.org/10.1111/bph.16180

Alexander, S. P. H., Kelly, E., Mathie, A. A., Peters, J. A., Veale, E. L., Armstrong, J. F., Buneman, O. P., Faccenda, E., Harding, S. D., Spedding, M., Cidlowski, J. A., Fabbro, D., Davenport, A. P., Striessnig, J., Davies, J. A., Ahlers-Dannen, K. E., Alqinyah, M., Arumugam, T. V., Bodle, C., … Zolghadri, Y. (2023). The Concise Guide to PHARMACOLOGY 2023/24: Introduction and Other Protein Targets. *British Journal of Pharmacology*, *180*, S1–S22. https://doi.org/10.1111/bph.16176

Alexander, S. P. H., Roberts, R. E., Broughton, B. R. S., Sobey, C. G., George, C. H., Stanford, S. C., Cirino, G., Docherty, J. R., Giembycz, M. A., Hoyer, D., Insel, P. A., Izzo, A. A., Ji, Y., MacEwan, D. J., Mangum, J., Wonnacott, S., & Ahluwalia, A. (2018). Goals and practicalities of immunoblotting and immunohistochemistry: A guide for submission to the British Journal of Pharmacology. *British Journal of Pharmacology*, *175*, 407–411. https://doi.org/10.1111/bph.14112

Berry, E. A., Huang, L. S., Lee, D. W., Daldal, F., Nagai, K., & Minagawa, N. (2010). Ascochlorin is a novel, specific inhibitor of the mitochondrial cytochrome bc1 complex. *Biochimica et Biophysica Acta*, *1797*(3), 360–370. https://doi.org/10.1016/j.bbabio.2009.12.003

Chen, T., Qiao, C., Yinwang, E., Wang, S., Wen, X., Feng, Y., Jin, X., Li, S., Xue, Y., Zhou, H., Zhang, W., Zeng, X., Wang, Z., Sun, H., Jiang, L., Li, H., Li, B., Cai, Z., Ye, Z., & Lin, N. (2024). Natural lung-tropic T(H)9 cells: A sharp weapon for established lung metastases. *Journal for Immunotherapy of Cancer*, *12*(12), e009629. https://doi.org/10.1136/jitc-2024-009629

Cho, H. J., Park, J. H., Nam, J. H., Chang, Y. C., Park, B., & Hoe, H. S. (2018). Ascochlorin suppresses MMP-2-mediated migration and invasion by targeting FAK and JAK-STAT signaling cascades. *Journal of Cellular Biochemistry*, *119*(1), 300–313. https://doi.org/10.1002/jcb.26179

Curtis, M. J., Alexander, S. P. H., Cortese-Krott, M., Kendall, D. A., Martemyanov, K. A., Mauro, C., Panettieri, R. A. Jr., Papapetropoulos, A., Patel, H. H., Santo, E. E., Schulz, R., Stefanska, B., Stephens, G. J., Teixeira, M. M., Vergnolle, N., Wang, X., & Ferdinandy, P. (2025). Guidance on the planning and reporting of experimental design and analysis. *British Journal of Pharmacology.*, *182*(7), 1413–1415. https://doi.org/10.1111/bph.17441

Dai, X., Ahn, K. S., Kim, C., Siveen, K. S., Ong, T. H., Shanmugam, M. K., Li, F., Shi, J., Kumar, A. P., Wang, L. Z., Goh, B. C., Magae, J., Hui, K. M., & Sethi, G. (2015). Ascochlorin, an isoprenoid antibiotic inhibits growth and invasion of hepatocellular carcinoma by targeting STAT3 signaling cascade through the induction of PIAS3. *Molecular Oncology*, *9*(4), 818–833. https://doi.org/10.1016/j.molonc.2014.12.008

Eikawa, S., Nishida, M., Mizukami, S., Yamazaki, C., Nakayama, E., & Udono, H. (2015). Immune-mediated antitumor effect by type 2 diabetes drug, metformin. *Proceedings of the National Academy of Sciences of the United States of America*, *112*(6), 1809–1814. https://doi.org/10.1073/pnas.1417636112

Finisguerra, V., Dvorakova, T., Formenti, M., Van Meerbeeck, P., Mignion, L., Gallez, B., & Van den Eynde, B. J. (2023). Metformin improves cancer immunotherapy by directly rescuing tumor-infiltrating CD8 T lymphocytes from hypoxia-induced immunosuppression. *Journal for Immunotherapy of Cancer*, *11*(5), e005719. https://doi.org/10.1136/jitc-2022-005719

Gan, X., Luo, X., Chen, J., Fang, W., Nie, M., Lu, H., Liu, Y., & Wang, X. (2025). Ilicicolin C suppresses the progression of prostate cancer by inhibiting PI3K/AKT/mTOR pathway. *Molecular and Cellular Biochemistry*, *480*(2), 1089–1104. https://doi.org/10.1007/s11010-024-05026-9

Hijikawa, Y., Matsuzaki, M., Suzuki, S., Inaoka, D. K., Tatsumi, R., Kido, Y., & Kita, K. (2017). Re-identification of the ascofuranone-producing fungus *Ascochyta viciae* as *Acremonium sclerotigenum*. *Journal of Antibiotics*, *70*(3), 304–307. https://doi.org/10.1038/ja.2016.132

Hong, S., Park, K. K., Magae, J., Ando, K., Lee, T. S., Kwon, T. K., Kwak, J. Y., Kim, C. H., & Chang, Y. C. (2005). Ascochlorin inhibits matrix metalloproteinase-9 expression by suppressing activator protein-1-mediated gene expression through the ERK1/2 signaling pathway: inhibitory effects of ascochlorin on the invasion of renal carcinoma cells. *Journal of Biological Chemistry*, *280*(26), 25202–25209. https://doi.org/10.1074/jbc.m413985200

Jeong, J. H., & Chang, Y. C. (2010). Ascochlorin, an isoprenoid antibiotic, induces G1 arrest via downregulation of c-Myc in a p53-independent manner. *Biochemical and Biophysical Research Communications*, *398*(1), 68–73. https://doi.org/10.1016/j.bbrc.2010.06.037

Jeong, J. H., Jeong, Y. J., Cho, H. J., Shin, J. M., Kang, J. H., Park, K. K., Chung, I. K., Chang, H. W., & Magae, J. (2012). Ascochlorin inhibits growth factor-induced HIF-1α activation and tumor-angiogenesis through the suppression of EGFR/ERK/p70S6K signaling pathway in human cervical carcinoma cells. *Journal of Cellular Biochemistry*, *113*(4), 1302–1313. https://doi.org/10.1002/jcb.24001

Jeong, J. H., Nakajima, H., Magae, J., Furukawa, C., Taki, K., Otsuka, K., Tomita, M., Lee, I. S., Kim, C. H., Chang, H. W., Min, K. S., Park, K. K.,

Park, K. K., & Chang, Y. C. (2009). Ascochlorin activates p53 in a manner distinct from DNA damaging agents. *International Journal of Cancer*, *124*(12), 2797–2803. https://doi.org/10.1002/ijc.24259

Jeong, Y. J., Hoe, H. S., Cho, H. J., Park, K. K., Kim, D. D., Kim, C. H., Magae, J., Kang, D. W., Lee, S. R., & Chang, Y. C. (2018). Suppression of c-Myc enhances $p21^{WAF1/CIP1}$-mediated G1 cell cycle arrest through the modulation of ERK phosphorylation by ascochlorin. *Journal of Cellular Biochemistry*, *119*(2), 2036–2047. https://doi.org/10.1002/jcb.26366

Khutornenko, A. A., Roudko, V. V., Chernyak, B. V., Vartapetian, A. B., Chumakov, P. M., & Evstafieva, A. G. (2010). Pyrimidine biosynthesis links mitochondrial respiration to the p53 pathway. *Proceedings of the National Academy of Sciences of the United States of America*, *107*(29), 12828–12833. https://doi.org/10.1073/pnas.0910885107

Lilley, E., Stanford, S. C., Kendall, D. E., Alexander, S. P. H., Cirino, G., Docherty, J. R., George, C. H., Insel, P. A., Izzo, A. A., Ji, Y., Panettieri, R. A., Sobey, C. G., Stefanska, B., Stephens, G., Teixeira, M., & Ahluwalia, A. (2020). ARRIVE 2.0 and the British Journal of Pharmacology: Updated guidance for 2020. *British Journal of Pharmacology*, *177*(16), 3611-3616. https://doi.org/10.1111/bph.15178

Lu, Y., Hong, B., Li, H., Zheng, Y., Zhang, M., Wang, S., Qian, J., & Yi, Q. (2014). Tumor-specific IL-9-producing $CD8^+$ Tc9 cells are superior effector than type-I cytotoxic Tc1 cells for adoptive immunotherapy of cancers. *Proceedings of the National Academy of Sciences of the United States of America*, *111*(6), 2265–2270. https://doi.org/10.1073/pnas.1317431111

Lu, Y., Hong, S., Li, H., Park, J., Hong, B., Wang, L., Zheng, Y., Liu, Z., Xu, J., He, J., Yang, J., Qian, J., & Yi, Q. (2012). Th9 cells promote antitumor immune responses in vivo. *Journal of Clinical Investigation*, *122*(11), 4160–4171. https://doi.org/10.1172/jci65459

Lu, Y., Wang, Q., Xue, G., Bi, E., Ma, X., Wang, A., Qian, J., Dong, C., & Yi, Q. (2018). Th9 cells represent a unique subset of $CD4^+$ T cells endowed with the ability to eradicate advanced tumors. *Cancer Cell*, *33*(6), e1047. https://doi.org/10.1016/j.ccell.2018.05.004

Lu, Y., Wang, Q., & Yi, Q. (2014). Anticancer Tc9 cells: Long-lived tumor-killing T cells for adoptive therapy. *Oncoimmunology*, *3*, e28542. https://doi.org/10.4161/onci.28542

Ma, X., Bi, E., Huang, C., Lu, Y., Xue, G., Guo, X., Wang, A., Yang, M., Qian, J., Dong, C., & Yi, Q. (2018). Cholesterol negatively regulates IL-9-producing $CD8^+$ T cell differentiation and antitumor activity. *Journal of Experimental Medicine*, *215*(6), 1555–1569. https://doi.org/10.1084/jem.20171576

Matsushita, H., Hosoi, A., Ueha, S., Abe, J., Fujieda, N., Tomura, M., Maekawa, R., Matsushima, K., Ohara, O., & Kakimi, K. (2015). Cytotoxic T lymphocytes block tumor growth both by lytic activity and IFNγ-dependent cell-cycle arrest. *Cancer Immunology Research*, *3*(1), 26–36. https://doi.org/10.1158/2326-6066.cir-14-0098

Moeller, J., Hultner, L., Schmitt, E., Breuer, M., & Dormer, P. (1990). Purification of MEA, a mast cell growth-enhancing activity, to apparent homogeneity and its partial amino acid sequencing. *Journal of Immunology*, *144*(11), 4231–4234. Retrieved from https://www.ncbi.nlm.nih.gov/pubmed/2140390

Murugaiyan, G., Beynon, V., Pires Da Cunha, A., Joller, N., & Weiner, H. L. (2012). IFN-γ limits Th9-mediated autoimmune inflammation through dendritic cell modulation of IL-27. *Journal of Immunology*, *189*(11), 5277–5283. https://doi.org/10.4049/jimmunol.1200808

Nishida, M., Yamashita, N., Ogawa, T., Koseki, K., Warabi, E., Ohue, T., Komatsu, M., Matsushita, H., Kakimi, K., Kawakami, E., Shiroguchi, K., & Udono, H. (2021). Mitochondrial reactive oxygen species trigger metformin-dependent antitumor immunity via activation of Nrf2/mTORC1/p62 axis in tumor-infiltrating CD8T lymphocytes. *Journal for Immunotherapy of Cancer*, *9*(9), e002954. https://doi.org/10.1136/jitc-2021-002954

Percie du Sert, N., Hurst, V., Ahluwalia, A., Alam, S., Avey, M. T., Baker, M., Browne, W. J., Clark, A., Cuthill, I. C., Dirnagl, U., Emerson, M., Garner, P., Holgate, S. T., Howells, D. W., Karp, N. A., Lazic, S. E., Lidster, K., MacCallum, C. J., Macleod, M., … Würbel, H. (2020). The ARRIVE guidelines 2.0: Updated guidelines for reporting animal research. *PLoS Biology*, *18*(7), e3000410. https://doi.org/10.1371/journal.pbio.3000410

Purwar, R., Schlapbach, C., Xiao, S., Kang, H. S., Elyaman, W., Jiang, X., Jetten, A. M., Khoury, S. J., Fuhlbrigge, R. C., Kuchroo, V. K., Clark, R. A., & Kupper, T. S. (2012). Robust tumor immunity to melanoma mediated by interleukin-9-producing T cells. *Nature Medicine*, *18*(8), 1248–1253. https://doi.org/10.1038/nm.2856

Sakaguchi, K., Nakajima, H., Mizuta, N., Furukawa, C., Ozawa, S., Ando, K., Chang, Y.-C., Yamagishi, H., & Magae, J. (2005). Selective cytotoxicity of ascochlorin in ER-negative human breast cancer cell lines. *Biochemical and Biophysical Research Communications*, *329*(1), 46–50. https://doi.org/10.1016/j.bbrc.2005.01.096

Sek, K., Chan, C. W., Beavis, P. A., & Darcy, P. K. (2021). Adoptive transfer of tumor-specific Th9 cells eradicates heterogeneous antigen-expressing tumor cells. *Cancer Cell*, *39*(12), 1564–1566. https://doi.org/10.1016/j.ccell.2021.10.013

Seok, J. Y., Jeong, Y. J., Hwang, S. K., Kim, C. H., Magae, J., & Chang, Y. C. (2018). Upregulation of AMPK by 4-O-methylascochlorin promotes autophagy via the HIF-1α expression. *Journal of Cellular and Molecular Medicine*, *22*(12), 6345–6356. https://doi.org/10.1111/jcmm.13933

Tamura, G., Suzuki, S., Takatsuki, A., Ando, K., & Arima, K. (1968). Ascochlorin, a new antibiotic, found by the paper-disc agar-diffusion method. I. Isolation, biological and chemical properties of ascochlorin. (Studies on antiviral and antitumor antibiotics. I). *Journal of Antibiotics*, *21*(9), 539–544. https://doi.org/10.7164/antibiotics.21.539

Uyttenhove, C., Simpson, R. J., & Van Snick, J. (1988). Functional and structural characterization of P40, a mouse glycoprotein with T-cell growth factor activity. *Proceedings of the National Academy of Sciences of the United States of America*, *85*(18), 6934–6938. https://doi.org/10.1073/pnas.85.18.6934

Visekruna, A., Ritter, J., Scholz, T., Campos, L., Guralnik, A., Poncette, L., Raifer, H., Hagner, S., Garn, H., Staudt, V., Bopp, T., Reuter, S., Taube, C., Loser, K., & Huber, M. (2013). Tc9 cells, a new subset of $CD8^+$ T cells, support Th2-mediated airway inflammation. *European Journal of Immunology*, *43*(3), 606–618. https://doi.org/10.1002/eji.201242825

Wherry, E. J. (2011). T cell exhaustion. *Nature Immunology*, *12*(6), 492–499. https://doi.org/10.1038/ni.2035

Zhang, Z., Li, F., Tian, Y., Cao, L., Gao, Q., Zhang, C., Zhang, K., Shen, C., Ping, Y., Maimela, N. R., Wang, L., Zhang, B., & Zhang, Y. (2020). Metformin enhances the antitumor activity of $CD8^+$ T lymphocytes via the AMPK-miR-107-Eomes-PD-1 pathway. *Journal of Immunology*, *204*(9), 2575–2588. https://doi.org/10.4049/jimmunol.1901213

SUPPORTING INFORMATION

Additional supporting information can be found online in the Supporting Information section at the end of this article.

How to cite this article: Imano, N., Nishida, M., Tokumasu, M., Zhao, W., Yamashita, N., & Udono, H. (2026). Induction of IL-9-producing $CD8^+$ T cells by ascochlorin derivatives. *British Journal of Pharmacology*, 1–17. https://doi.org/10.1111/bph.70316